

## SUPPORTING INFORMATION

### A combined experimental and theoretical study of the thermal cycloaddition of aryl azides with activated alkenes

Sarah Zeghada, Ghenia Bentabed-Ababsa, Aïcha Derdour, Safer Abdelmounim,  
Luis R. Domingo, José A. Sáez, Thierry Roisnel, Ekhllass Nassar and Florence Mongin

#### Index

	Page
<b>Table S1.</b> B3LYP/6-31G* Total energies in gas phase and in solution, of the stationary points involved in the thermal domino reactions of the $\beta$ -dicarbonyl compounds <b>2</b> with the phenyl azides <b>1</b> .	1
<b>Table S2.</b> B3LYP/6-311+G** Total (E, in au.) and relative energies ( $\Delta E$ , in kcal/mol) in gas phase and in solution, of the stationary points involved in the thermal domino reactions of the $\beta$ -dicarbonyl compounds <b>2</b> with the phenyl azides <b>1</b> .	2
<b>Table S3.</b> B3LYP/6-311+G** Lengths (in angstroms), asynchronicity ( $\Delta t$ ), charge transfer (CT, in e), and bond orders (BO) of the C-N forming bonds involved in the 32CA reactions between the enols <b>2'</b> and the phenyl azides <b>1</b> .	3
<b>Table S4.</b> B3LYP/6-311+G** Lengths of the breaking and forming bonds (in angstroms) at the TSs involved in the water elimination.	3
<b>Figure S1.</b> B3LYP/6-31G* Transition states involved in the regioisomeric channels 1 and 2 associated with the 13DC reaction between the enol <b>2'a-Z</b> and phenyl azide ( <b>1e</b> ).	4
<b><sup>1</sup>H and <sup>13</sup>C NMR spectra.</b> Compounds <b>3a-h</b> , <b>5a,b</b> , <b>8</b> and <b>10</b> .	5
<b>X-Ray diagrams.</b> Compounds <b>3b,c,f</b> and <b>5a</b>	17

**Table S1.** B3LYP/6-31G\* Total energies in gas phase and in solution, of the stationary points involved in the thermal domino reactions of the  $\beta$ -dicarbonyl compounds **2** with the phenyl azides **1**.

	E	Esolv
<b>1</b>	-600.339478	-600.351888
<b>1e</b>	-395.838293	-395.845107
<b>2a</b>	-345.783930	-345.798120
<b>2'a-Z</b>	-345.799880	-345.806354
<b>2'a-E</b>	-345.781300	-345.796587
<b>2b</b>	-421.025418	-421.034564
<b>2'b-Z</b>	-421.028507	-421.034809
<b>2'b-E</b>	-421.012961	-421.027779
<b>TS11ea</b>	-741.600612	-741.612040
<b>TS12ea</b>	-741.587347	-741.600954
<b>6ea</b>	-741.643397	-741.656283
<b>6ea</b>	-741.638813	-741.658358
<b>TS11a</b>	-946.106113	-946.122814
<b>TS12a</b>	-946.087754	-946.106151
<b>61a</b>	-946.146725	-946.164719
<b>62a</b>	-946.142062	-946.166785
<b>TS11b</b>	-1021.334266	-1021.351315
<b>TS12b</b>	-1021.320116	-1021.337592
<b>61b</b>	-1021.377031	-1021.395400
<b>62b</b>	-1021.376075	-1021.397792
<b>IN11a</b>	-1120.965805	-1121.050323
<b>IN12a</b>	-1120.956200	-1121.038231
<b>TS21a</b>	-1120.959295	-1121.041749
<b>TS22a</b>	-1120.948580	-1121.032334
<b>31a</b>	-869.748115	-869.766034
<b>32b</b>	-869.736532	-869.755960
<b>IN11b</b>	-1196.196328	-1196.281071
<b>IN12b</b>	-1196.190484	-1196.272085
<b>TS21b</b>	-1196.190990	-1196.272255
<b>TS22b</b>	-1196.185951	-1196.265085
<b>31b</b>	-944.974472	-944.994347
<b>32b</b>	-944.970063	-944.988637

**Table S2.** B3LYP/6-311+G\*\* Total (E, in au.) and relative energies ( $\Delta E$ , in kcal/mol) in gas phase and in solution, of the stationary points involved in the thermal domino reactions of the  $\beta$ -dicarbonyl compounds **2** with the phenyl azides **1**.

	E	$\Delta E$	Esolv	$\Delta E_{\text{solv}}$
<b>1</b>	-600.506010		-600.520865	
<b>1e</b>	-395.943084		-395.951121	
<b>2a</b>	-345.890473		-345.890473	
<b>2'a-Z</b>	-345.911074	-12.9	-345.911074	-7.2
<b>2'a-E</b>	-345.893729	-2.0	-345.893729	-2.1
<b>2b</b>	-421.156795		-421.156795	
<b>2'b-Z</b>	-421.163543	-4.2	-421.163543	-2.2
<b>2'b-E</b>	-421.149430	4.6	-421.149430	1.2
<b>TS11ea</b>	-741.811345	26.9	-741.825137	28.2
<b>TS12ea</b>	-741.798498	34.9	-741.814887	34.7
<b>6ea</b>	-741.846959	4.5	-741.865055	3.2
<b>6ea</b>	-741.848999	3.2	-741.871886	-1.1
<b>TS11a</b>	-946.378068	24.5	-946.397931	26.3
<b>TS12a</b>	-946.360917	35.3	-946.383078	35.6
<b>61a</b>	-946.416262	0.5	-946.437569	1.4
<b>62a</b>	-946.413912	2.0	-946.443010	-2.0
<b>TS11b</b>	-1021.630101	20.5	-1021.650338	23.9
<b>TS12b</b>	-1021.616738	28.9	-1021.637672	31.9
<b>61b</b>	-1021.670566	-4.9	-1021.692365	-2.5
<b>62b</b>	-1021.670825	-5.0	-1021.697461	-5.7
<b>IN11a</b>	-1121.283449		-1121.371536	
<b>IN12a</b>	-1121.273672		-1121.359182	
<b>TS21a</b>	-1121.277386	3.8	-1121.362875	5.4
<b>TS22a</b>	-1121.266585	4.5	-1121.354225	3.1
<b>31a</b>	-869.984287	-16.1	-870.005820	-23.7
<b>32b</b>	-869.973009	-9.0	-869.995799	-17.4
<b>IN11b</b>	-1196.537390		-1196.625392	
<b>IN12b</b>	-1196.531042		-1196.625392	
<b>TS21b</b>	-1196.532351	3.2	-1196.616796	5.4
<b>TS22b</b>	-1196.526985	2.6	-1196.612751	7.9
<b>31b</b>	-945.234333	-18.8	-945.257916	-25.9
<b>32b</b>	-945.229914	-16.1	-945.251972	-22.2

**Table S3.** B3LYP/6-311+G\*\* Lengths (in angstroms), asynchronicity ( $\Delta l$ ), charge transfer (CT, in e), and bond orders (BO) of the C-N forming bonds involved in the 32CA reactions between the enols **2'** and the phenyl azides **1**.

	N1-C5(4)	N3-C4(5)	$\Delta l$	CT	BO N1-C5(4)	BO N3-C4(5)
<b>TS11ea</b>	1.998	2.157	0.16	-0.18	0.47	0.31
<b>TS12ea</b>	1.885	2.155	0.27	-0.09	0.50	0.35
<b>TS11a</b>	1.952	2.228	0.28	-0.27	0.50	0.27
<b>TS12a</b>	1.892	2.135	0.24	-0.14	0.50	0.36
<b>TS11b</b>	1.957	2.240	0.28	-0.27	0.50	0.26
<b>TS12b</b>	1.935	2.128	0.19	-0.16	0.47	0.36

**Table S4.** B3LYP/6-311+G\*\* Lengths of the breaking and forming bonds (in angstroms) at the TSs involved in the water elimination.

	C4-O6	O8-H7	H7-O6	H9-N10
<b>TS21a</b>	1.629	1.286	1.129	2.037
<b>TS22a</b>	1.700	1.550	1.019	2.244
<b>TS21b</b>	1.621	1.268	1.142	1.983
<b>TS22b</b>	1.747	1.542	1.021	2.140

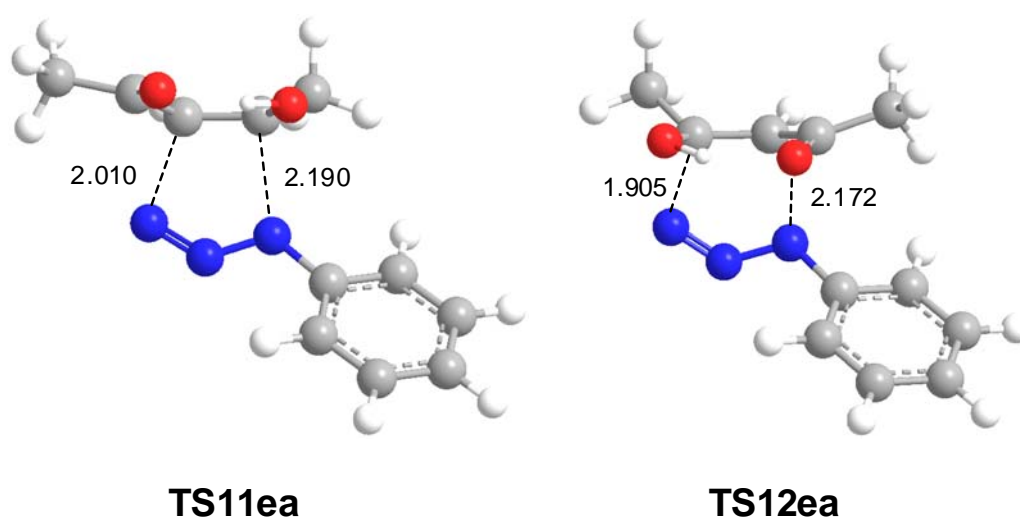
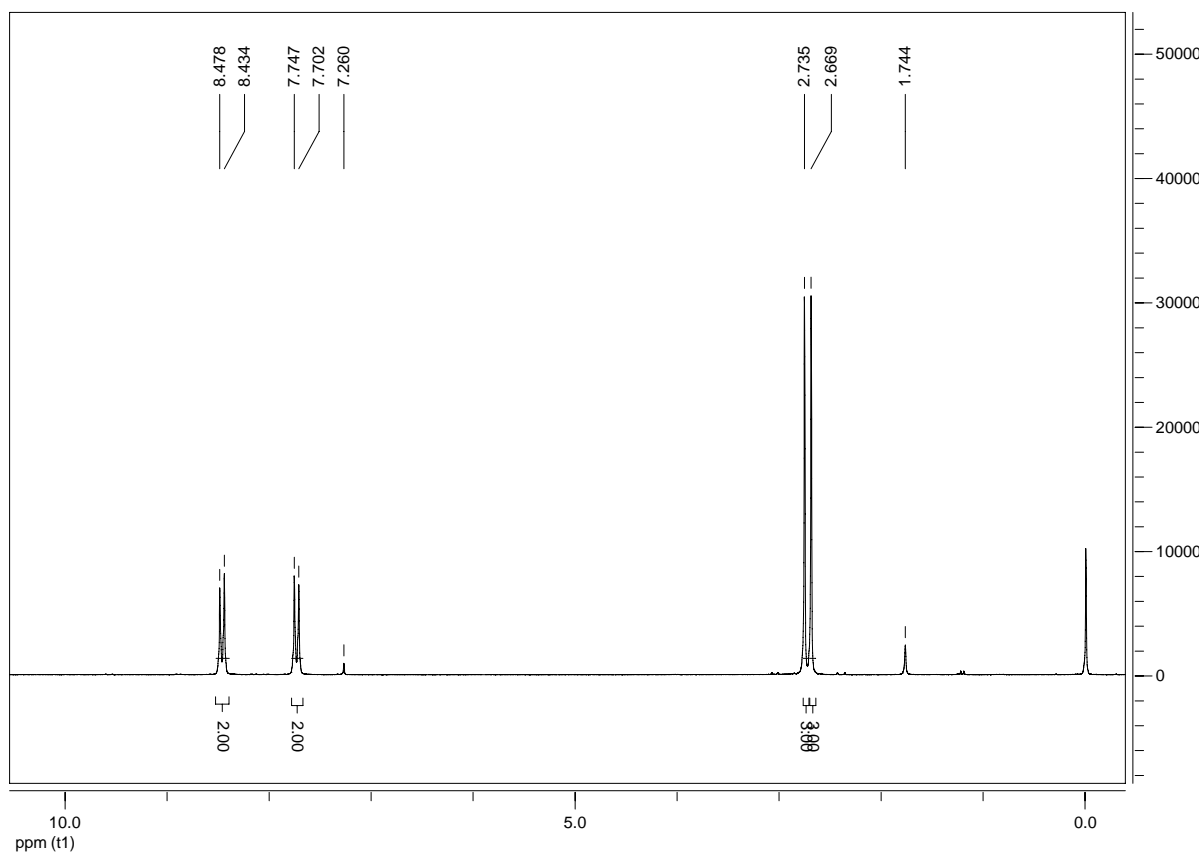


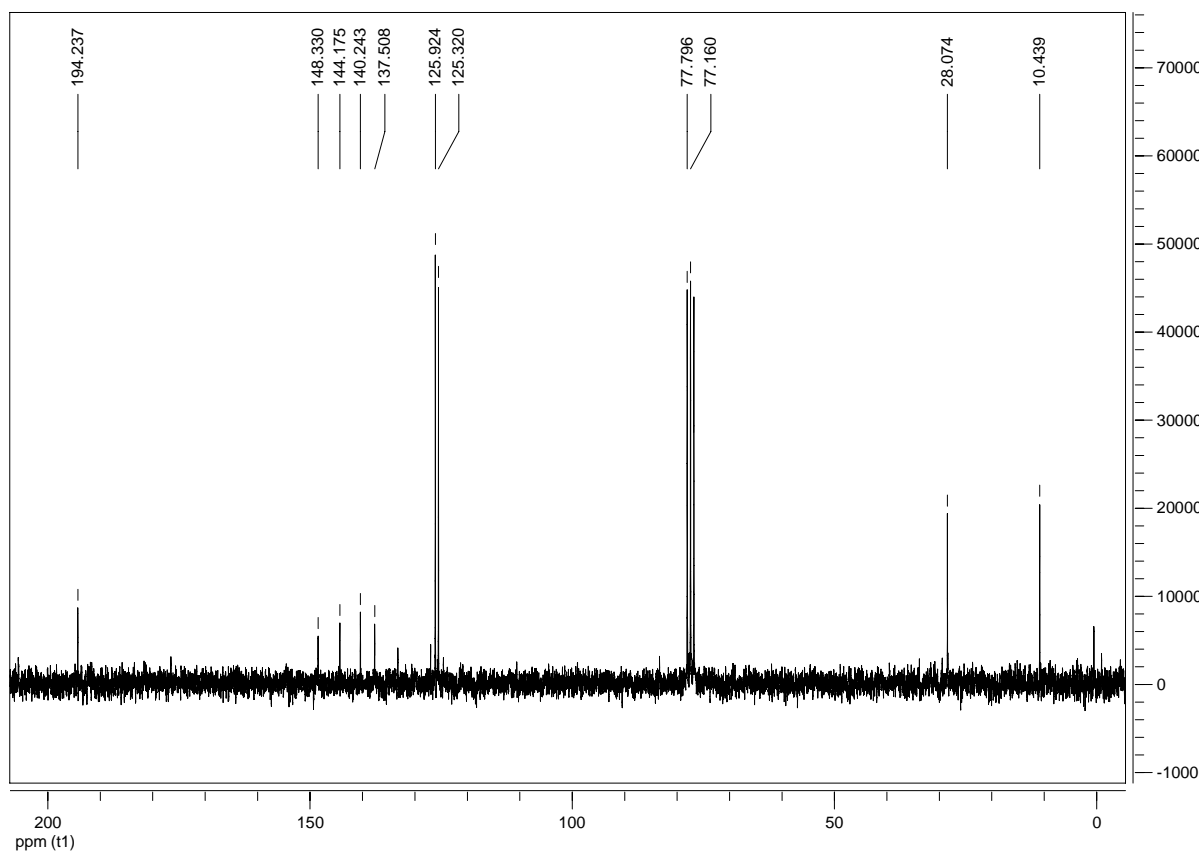
**Figure S1.** B3LYP/6-31G\* Transition states involved in the regioisomeric channels 1 and 2 associated with the 13DC reaction between the enol **2'a-Z** and phenyl azide (**1e**).

### Compound 3a

$^1\text{H}$  NMR (300 MHz,  $\text{CDCl}_3$ ):

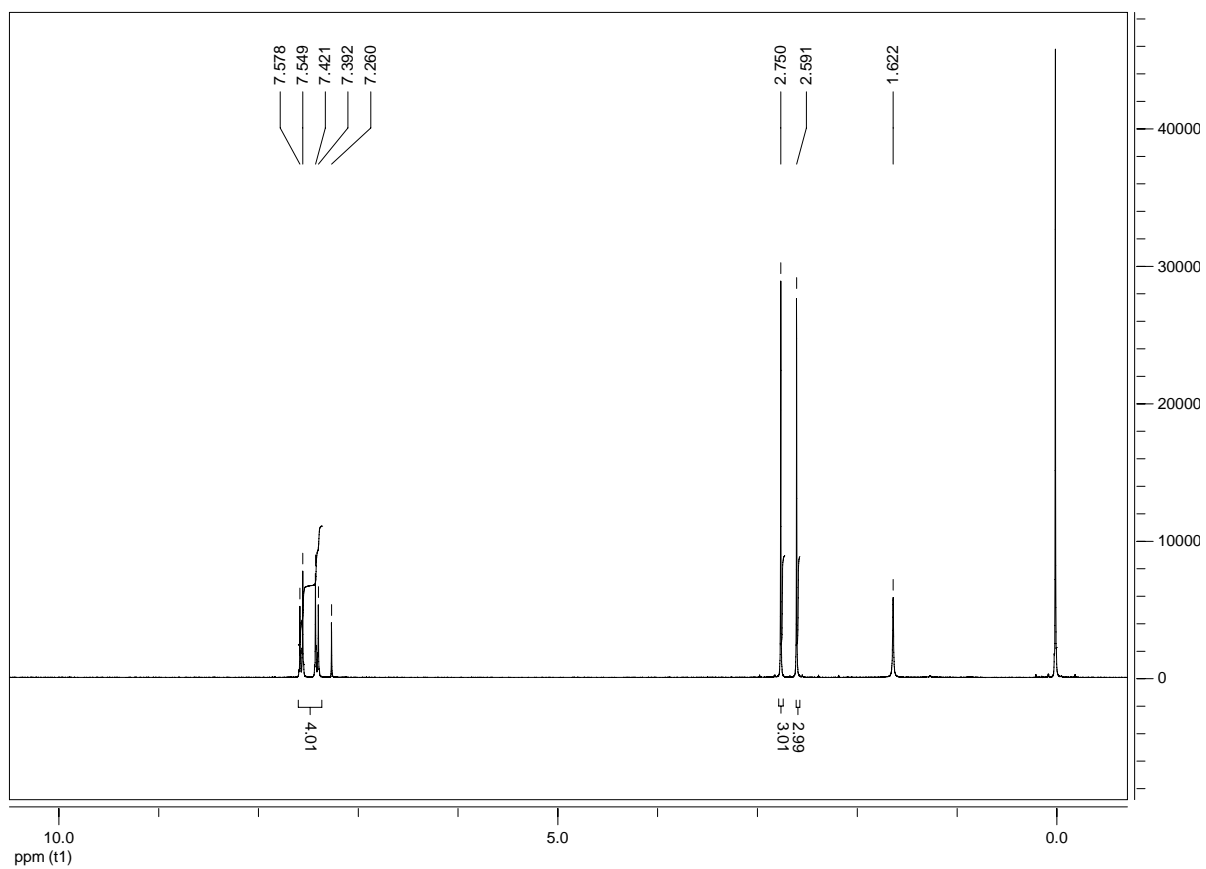


$^{13}\text{C}$  NMR (75 MHz,  $\text{CDCl}_3$ ):

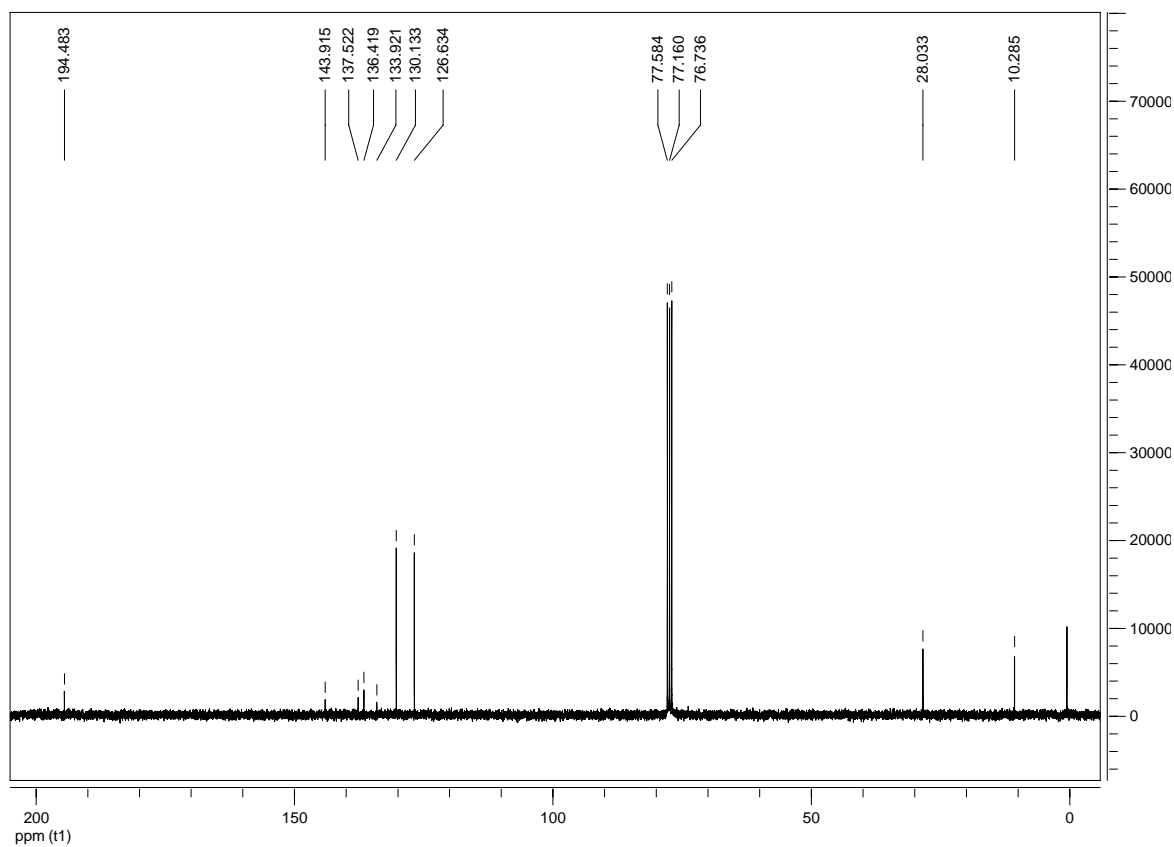


### Compound 3b

$^1\text{H}$  NMR (300 MHz,  $\text{CDCl}_3$ ):

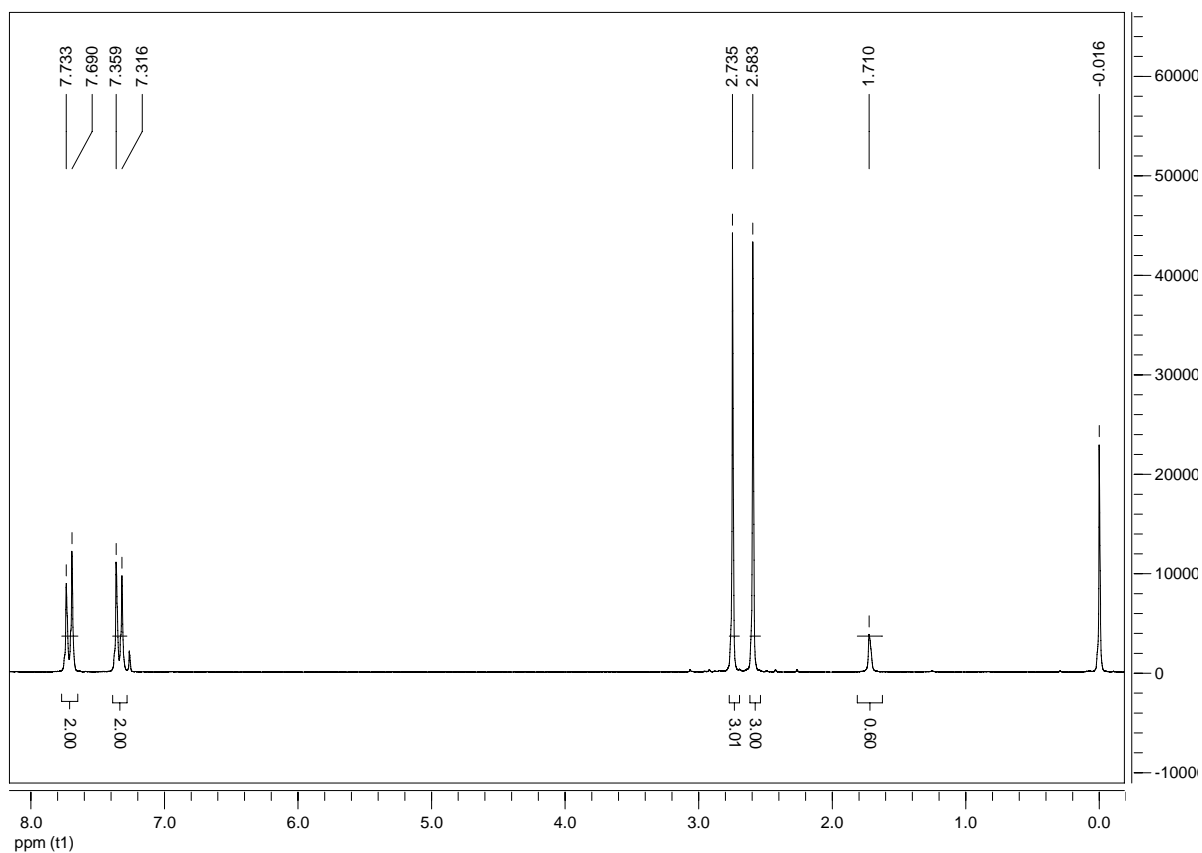


$^{13}\text{C}$  NMR (75 MHz,  $\text{CDCl}_3$ ):

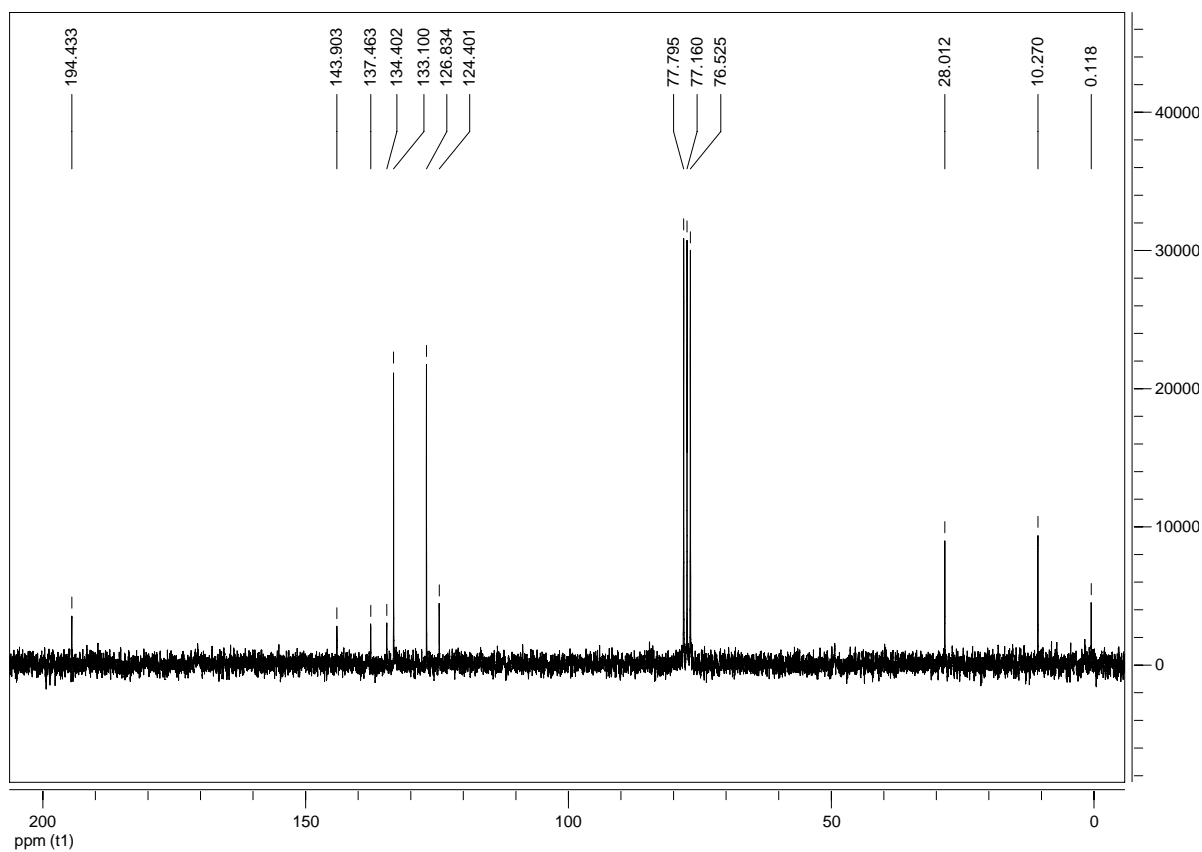


### Compound 3c

$^1\text{H}$  NMR (300 MHz,  $\text{CDCl}_3$ ):



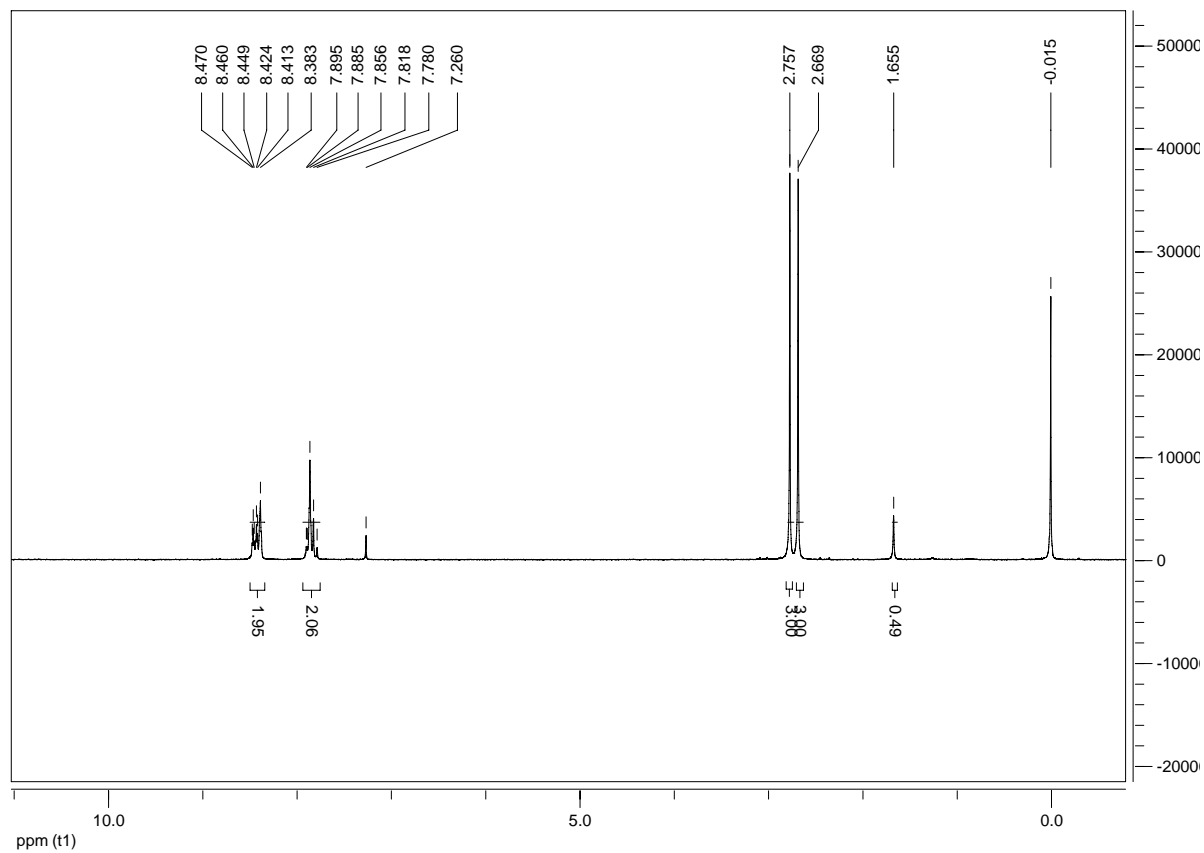
$^{13}\text{C}$  NMR (75 MHz,  $\text{CDCl}_3$ ):



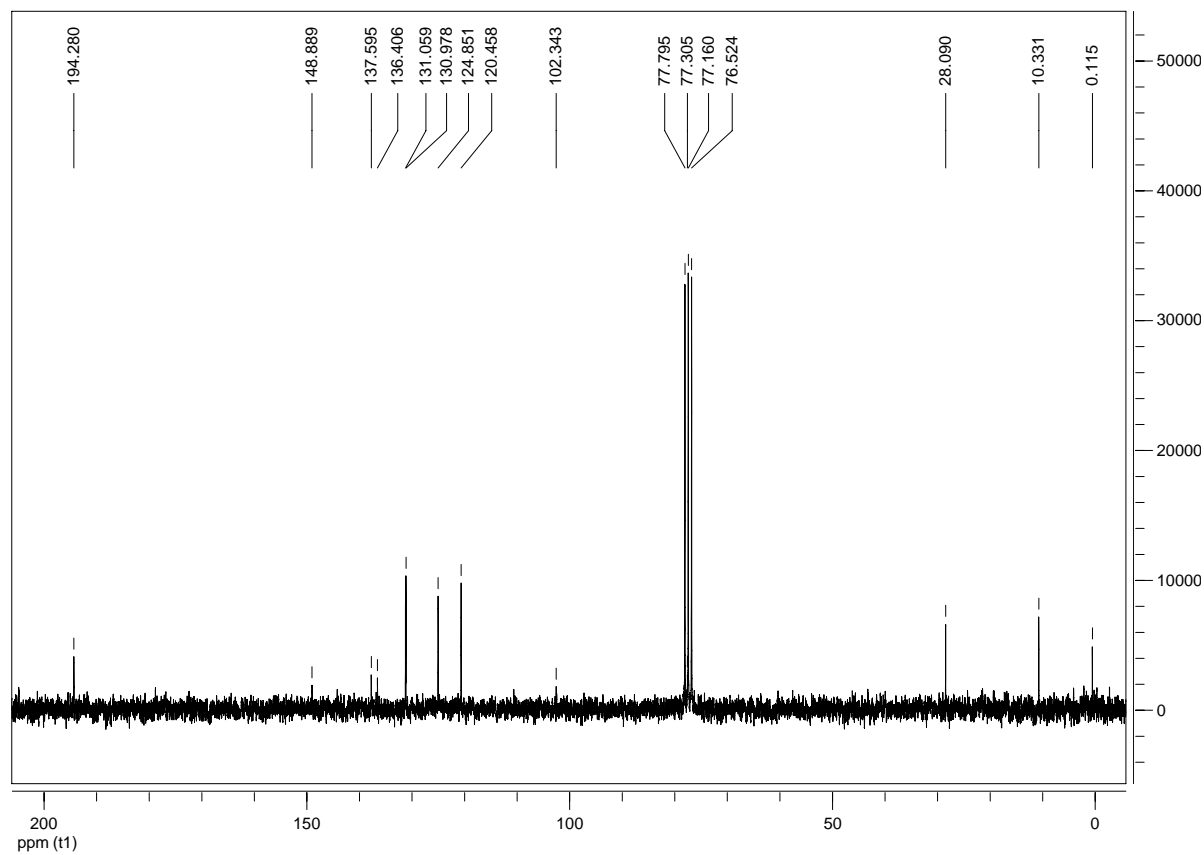


### Compound 3d

$^1\text{H}$  NMR (300 MHz,  $\text{CDCl}_3$ ):

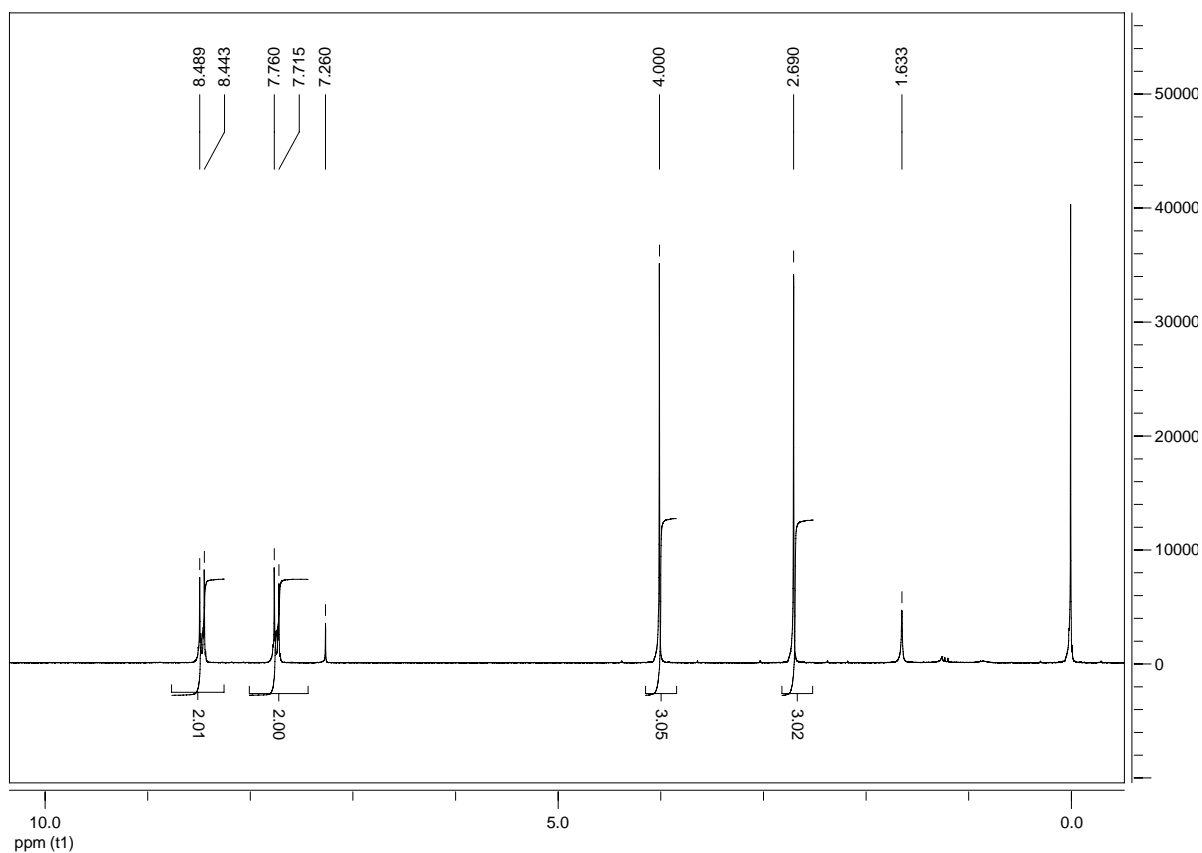


$^{13}\text{C}$  NMR (75 MHz,  $\text{CDCl}_3$ ):

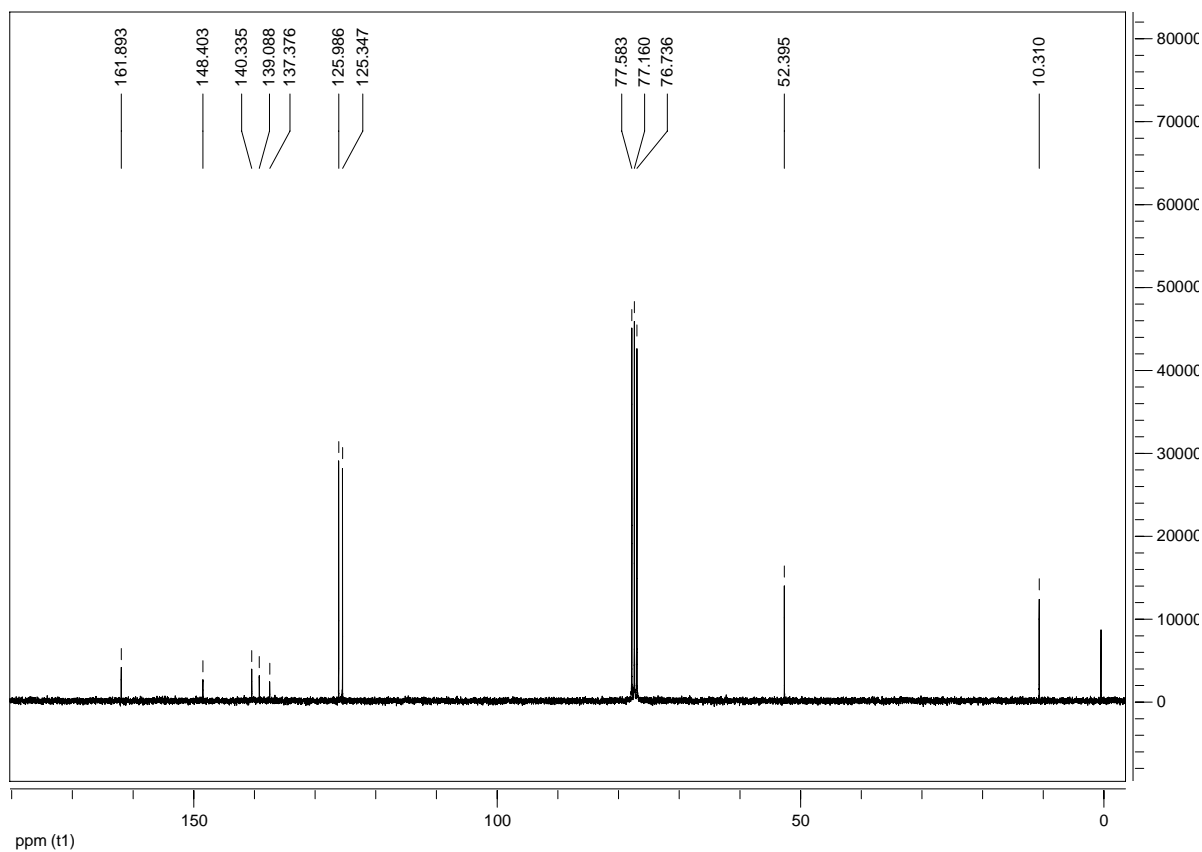


### Compound 3e

$^1\text{H}$  NMR (300 MHz,  $\text{CDCl}_3$ ):

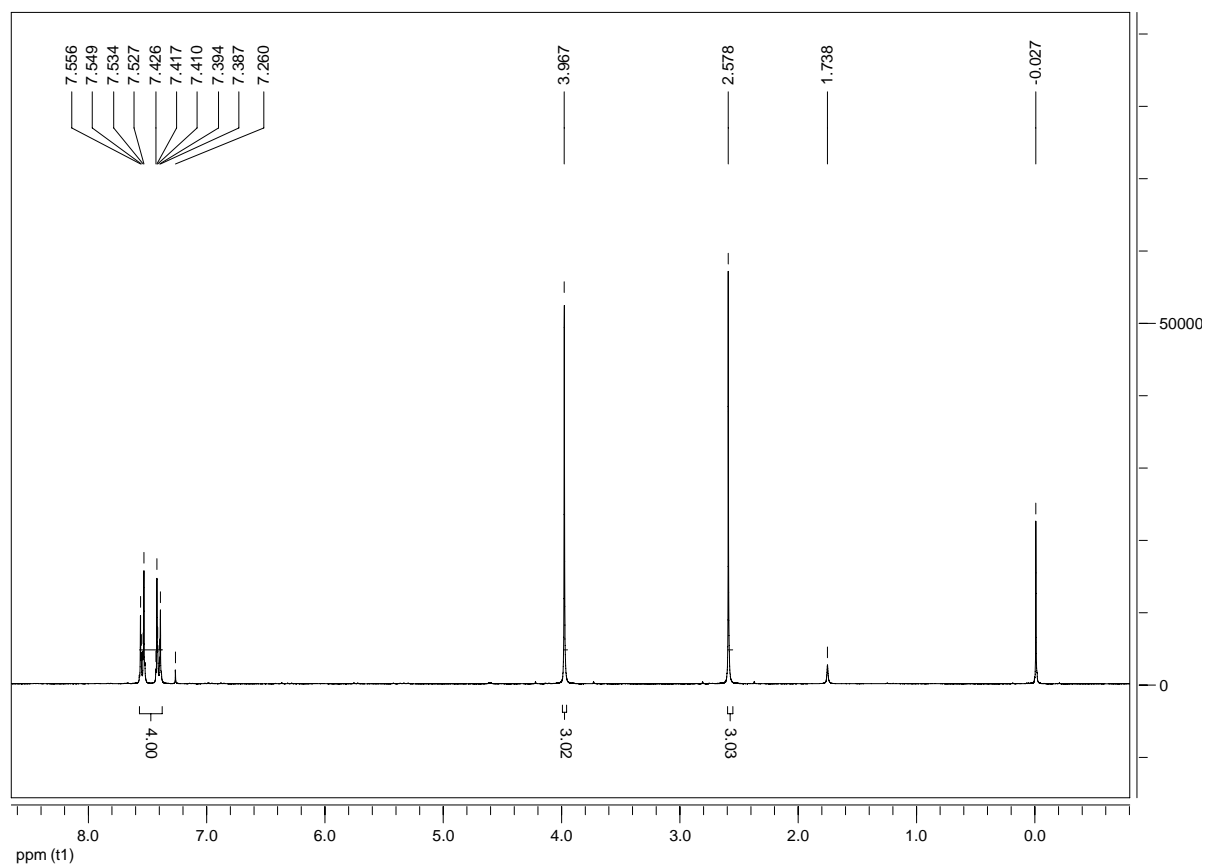


$^{13}\text{C}$  NMR (75 MHz,  $\text{CDCl}_3$ ):

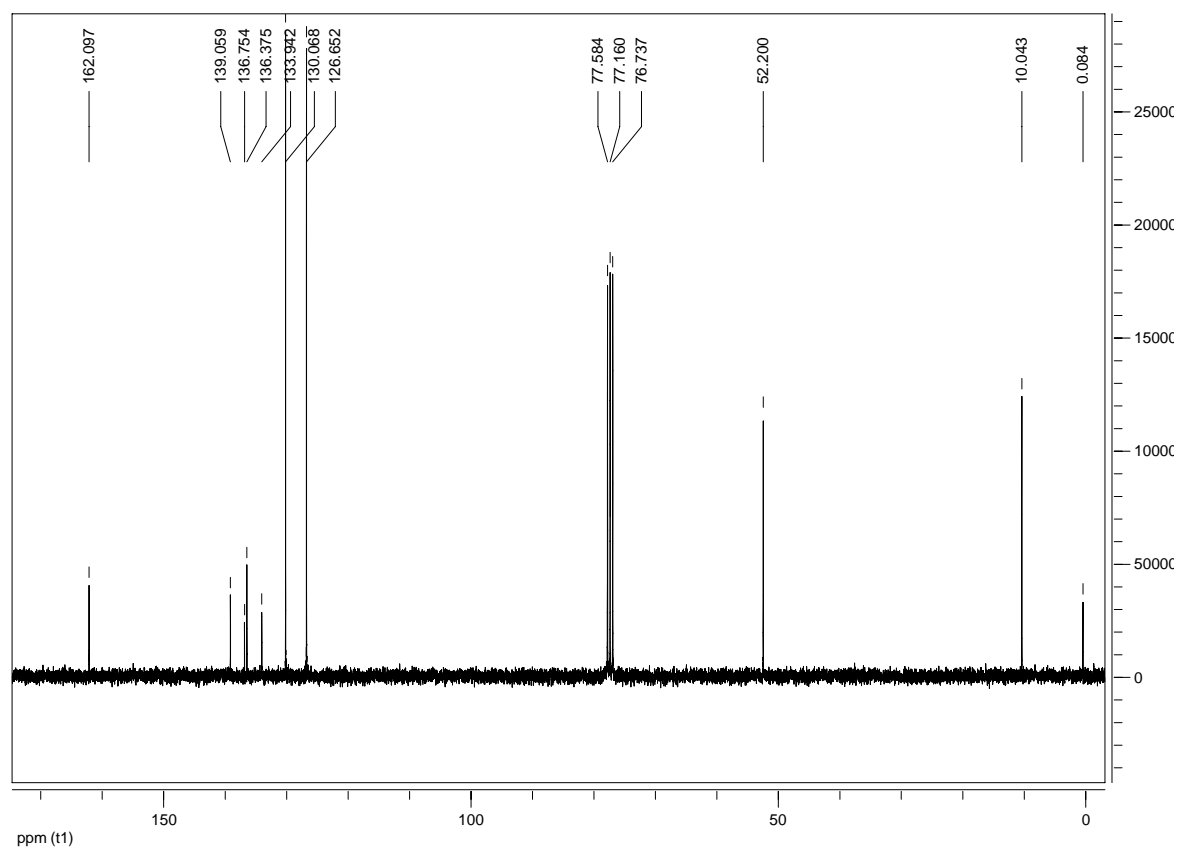


### Compound **3f**

$^1\text{H}$  NMR (300 MHz,  $\text{CDCl}_3$ ):

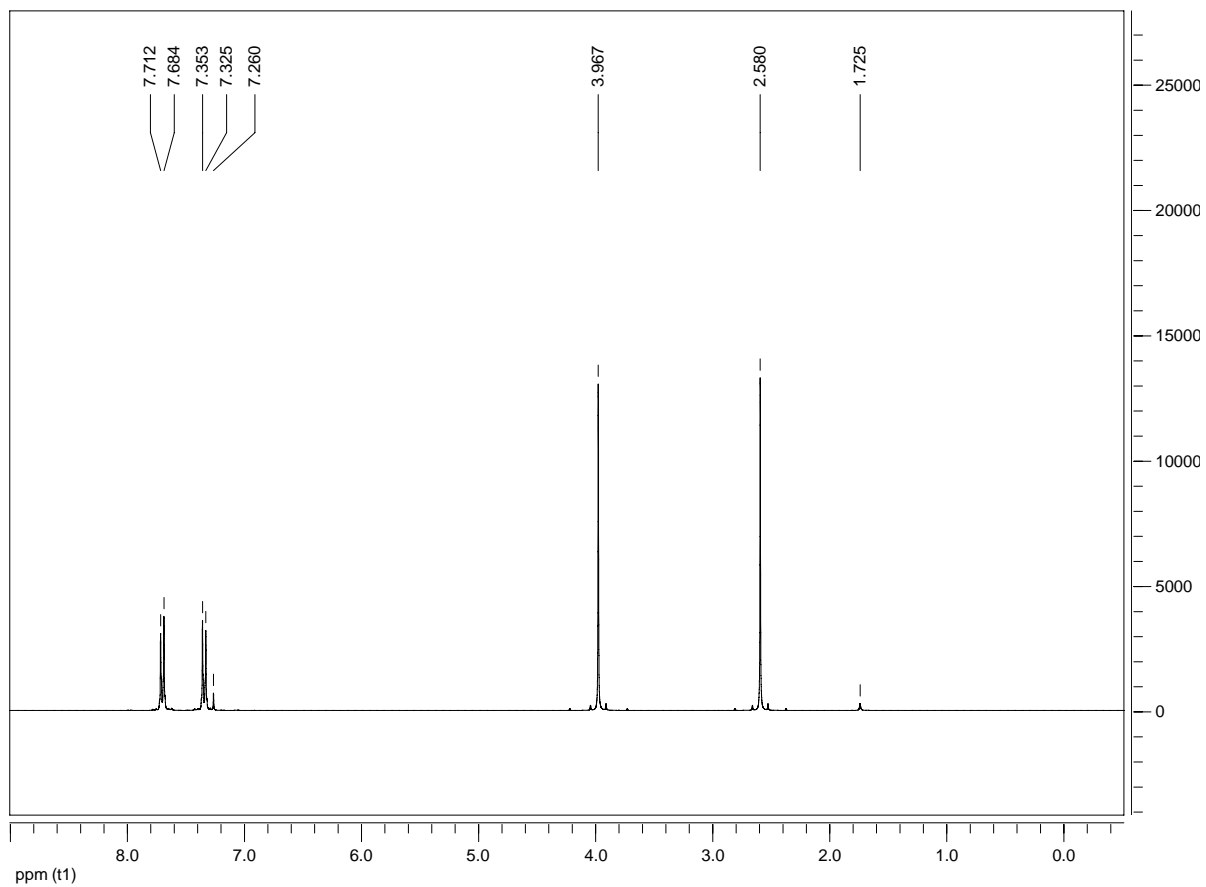


$^{13}\text{C}$  NMR (75 MHz,  $\text{CDCl}_3$ ):

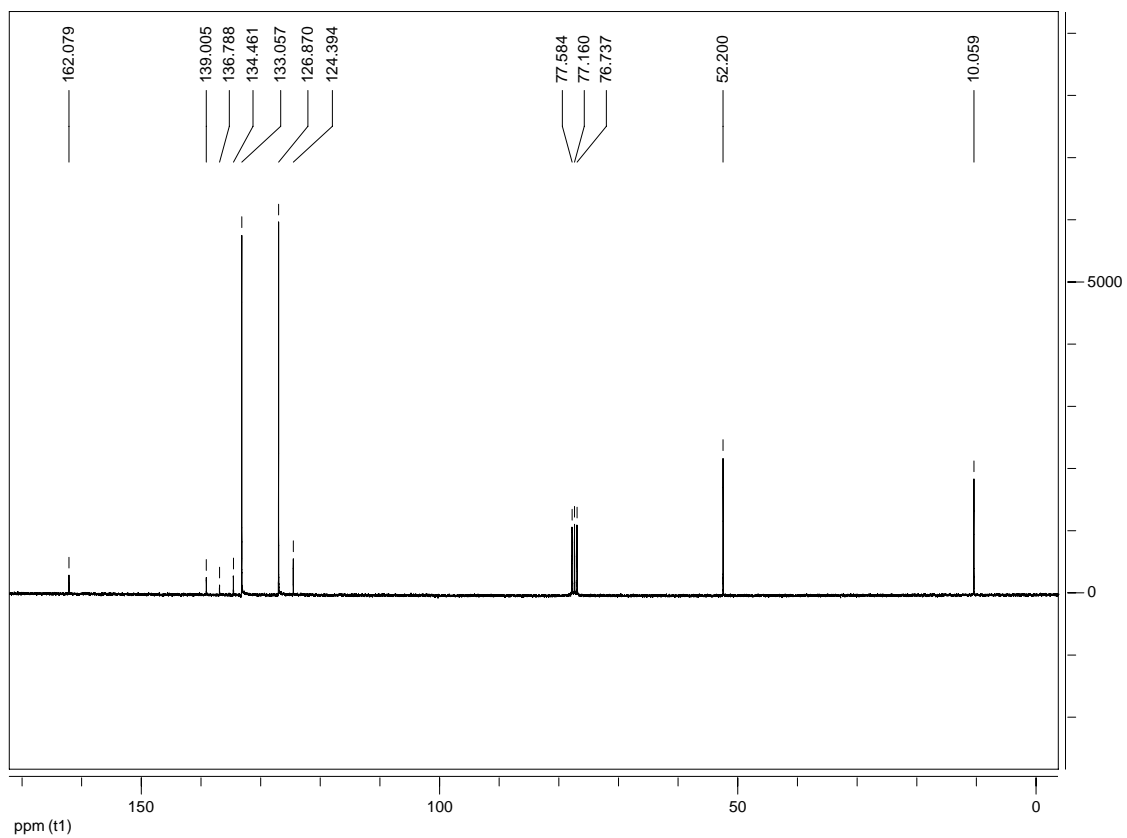


### Compound 3g

$^1\text{H}$  NMR (300 MHz,  $\text{CDCl}_3$ ):

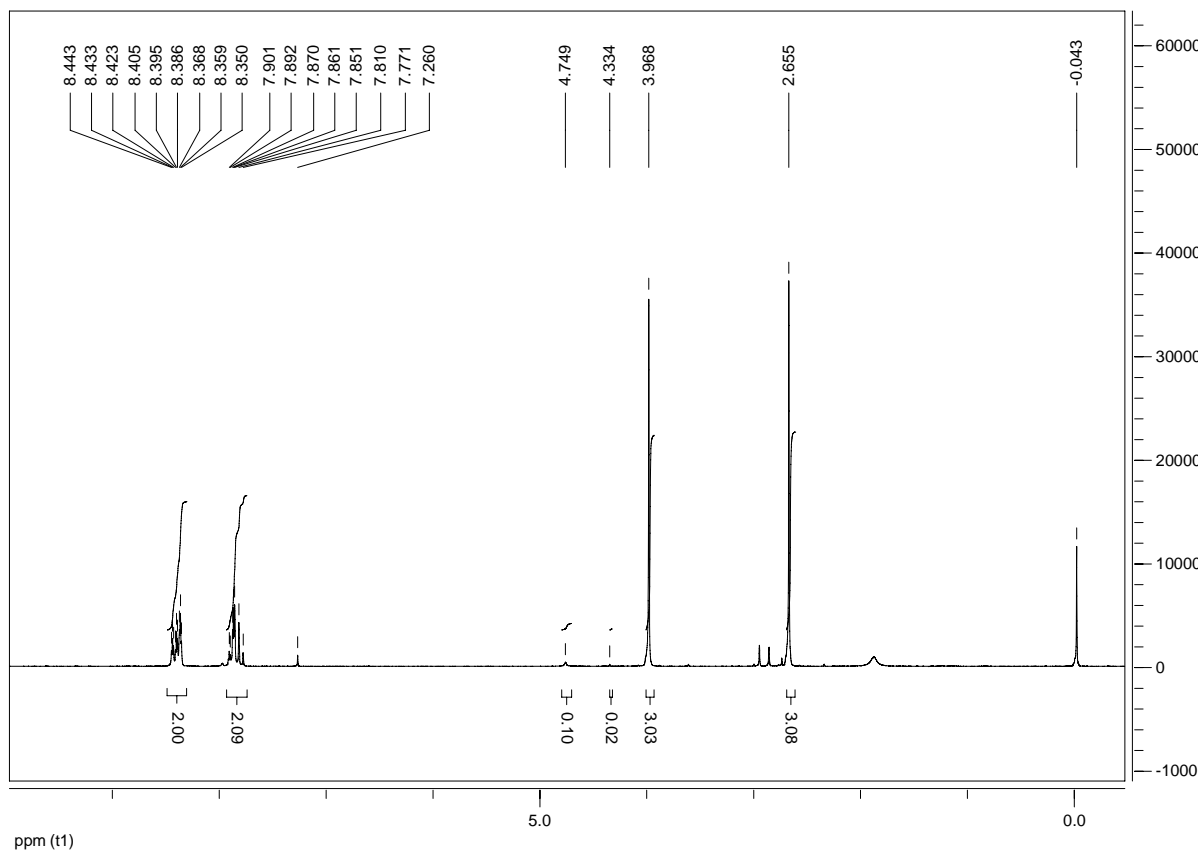


$^{13}\text{C}$  NMR (75 MHz,  $\text{CDCl}_3$ ):

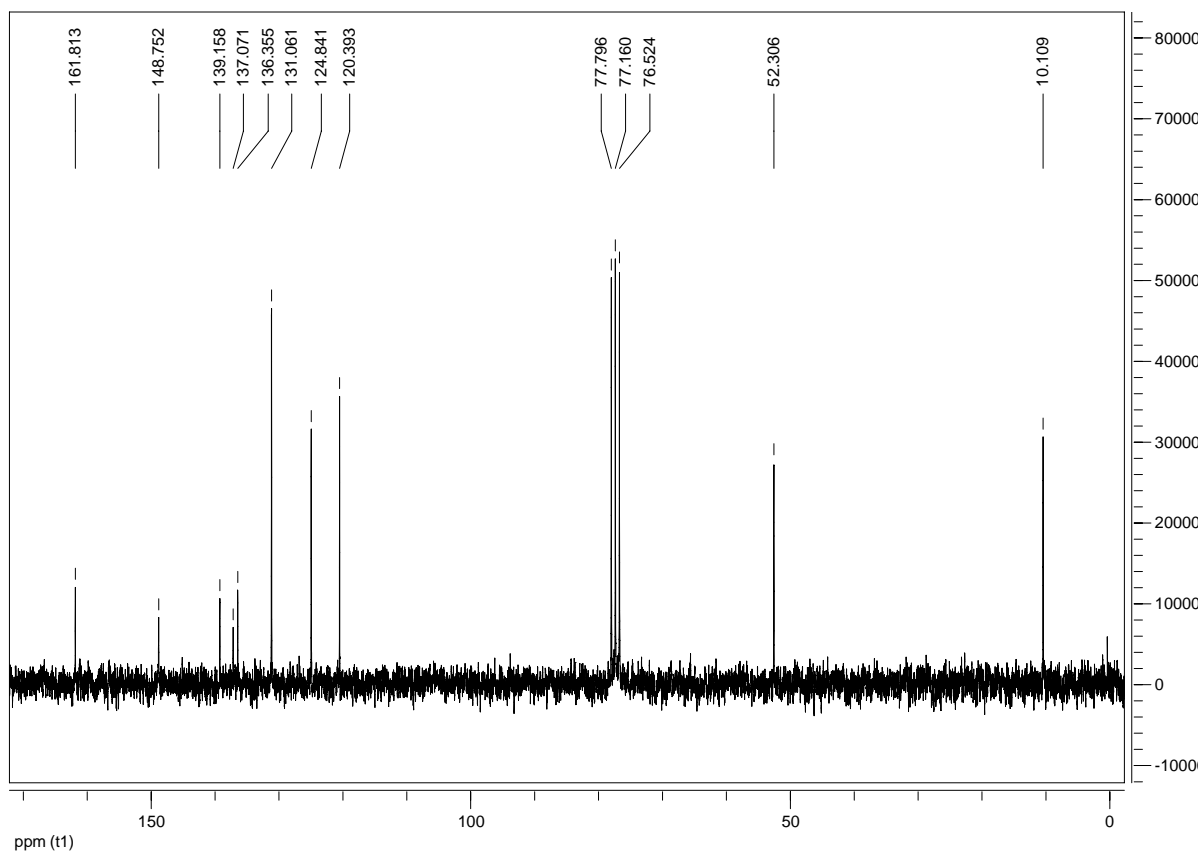


### Compound 3h

$^1\text{H}$  NMR (300 MHz,  $\text{CDCl}_3$ ):

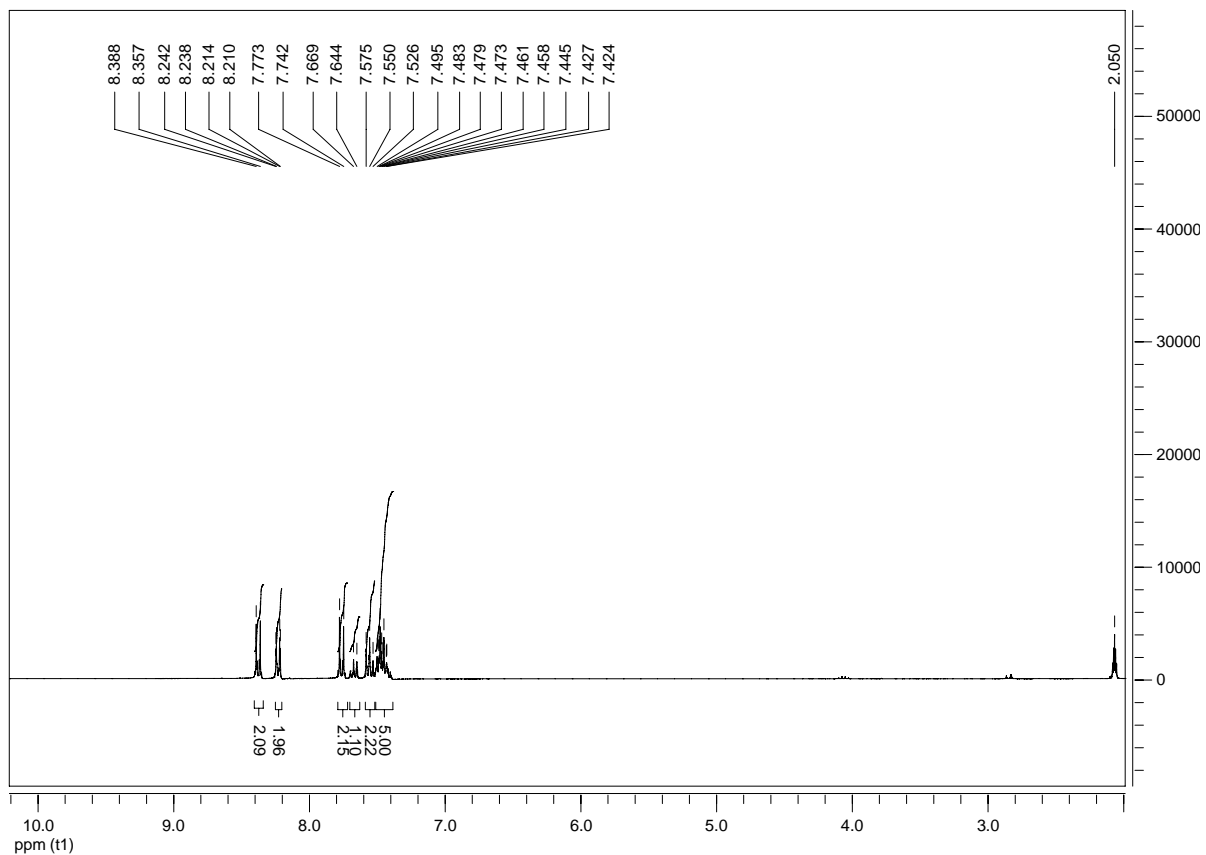


$^{13}\text{C}$  NMR (75 MHz,  $\text{CDCl}_3$ ):

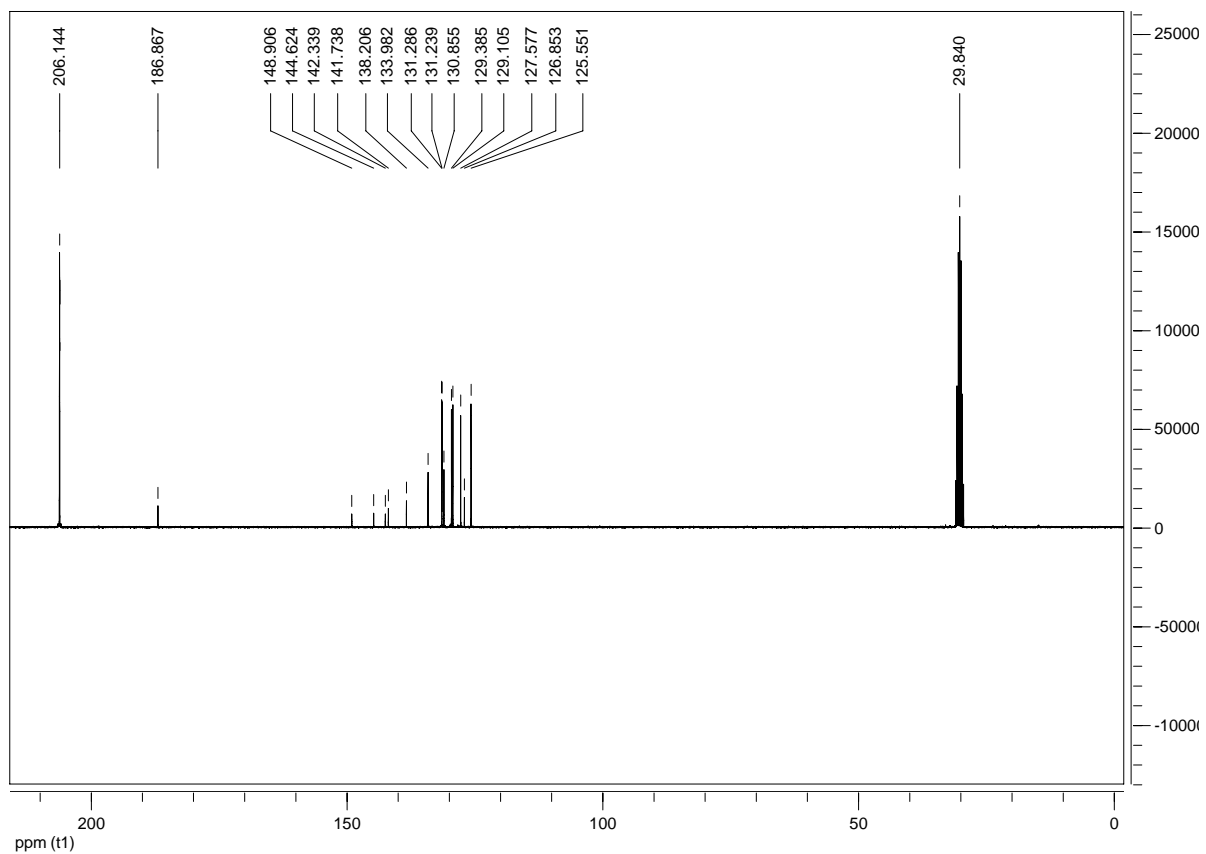


### Compound 5a

$^1\text{H}$  NMR (300 MHz,  $(\text{CD}_3)_2\text{CO}$ ):

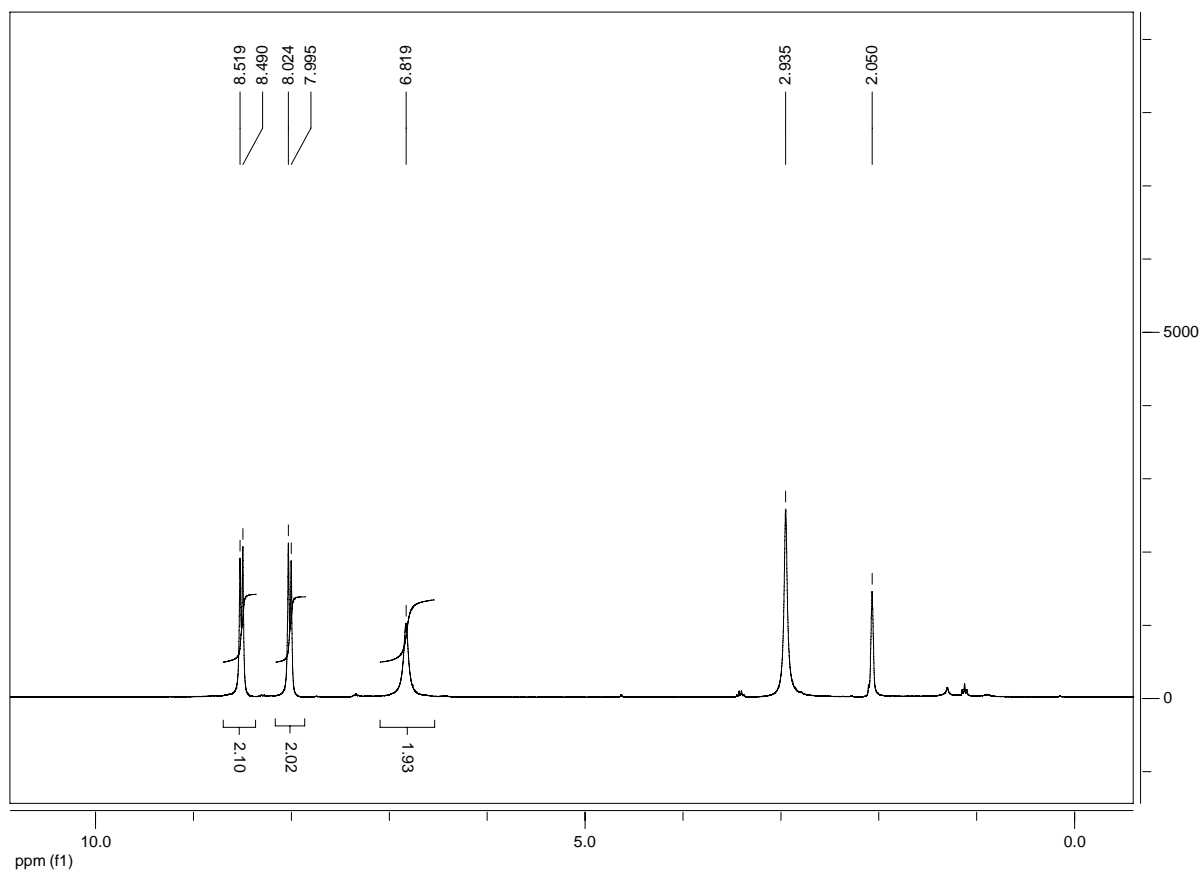


$^{13}\text{C}$  NMR (75 MHz,  $(\text{CD}_3)_2\text{CO}$ ):

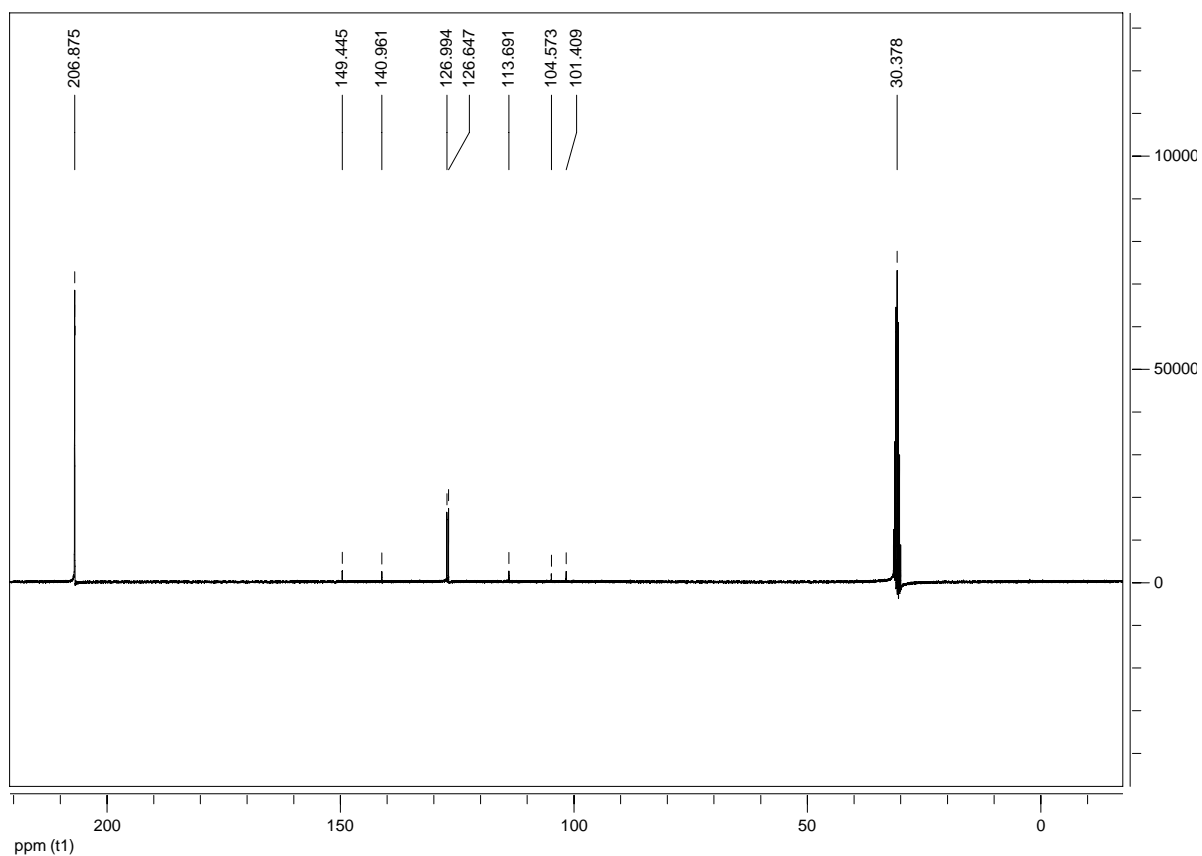


### Compound 5b

$^1\text{H}$  NMR (300 MHz,  $(\text{CD}_3)_2\text{CO}$ ):

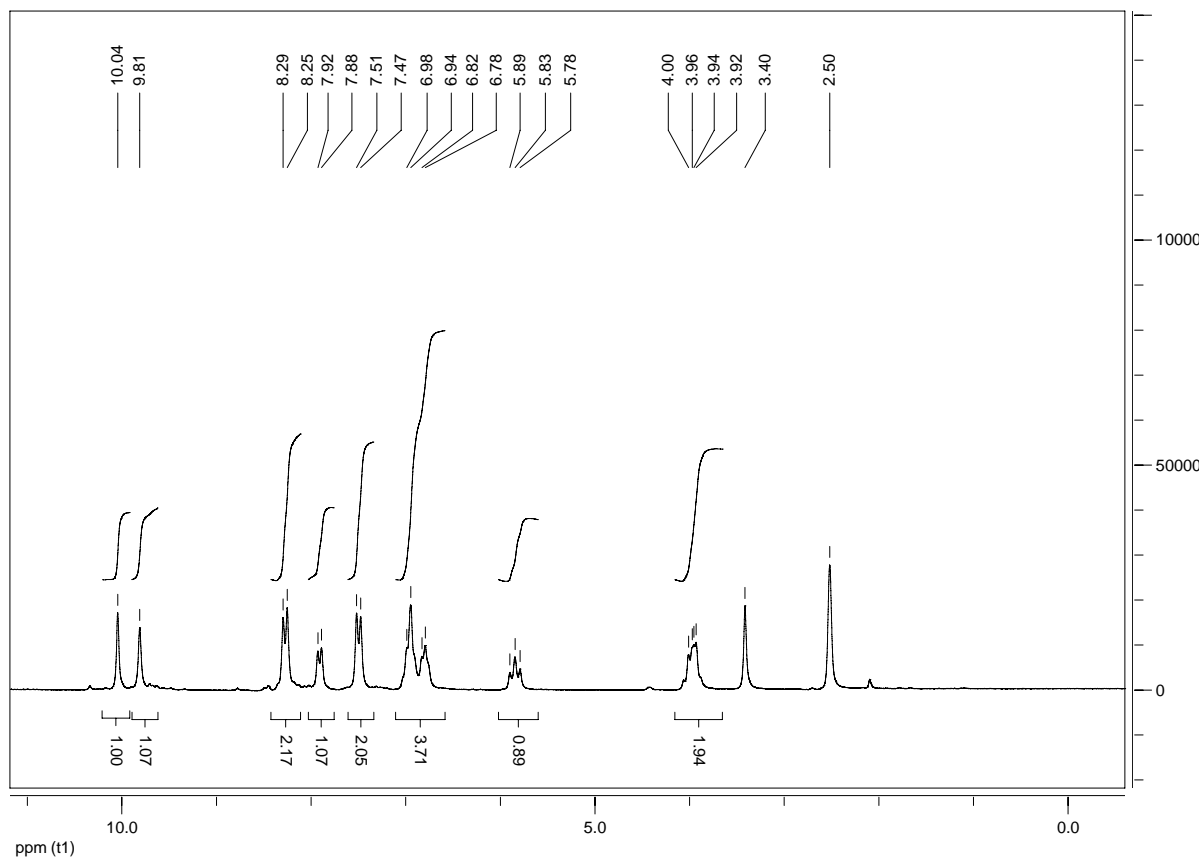


$^{13}\text{C}$  NMR (75 MHz,  $(\text{CD}_3)_2\text{CO}$ ):

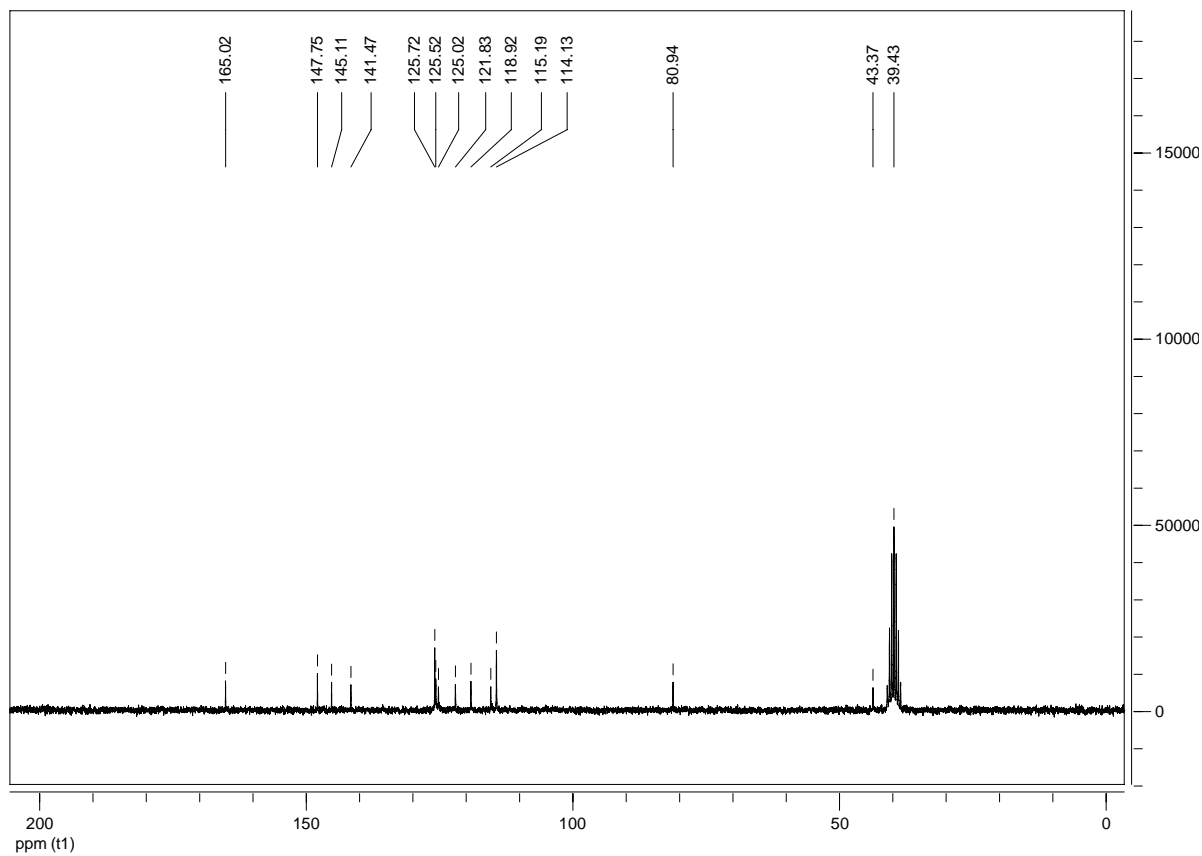


### Compound 8

$^1\text{H}$  NMR (200 MHz,  $(\text{CD}_3)_2\text{SO}$ ):



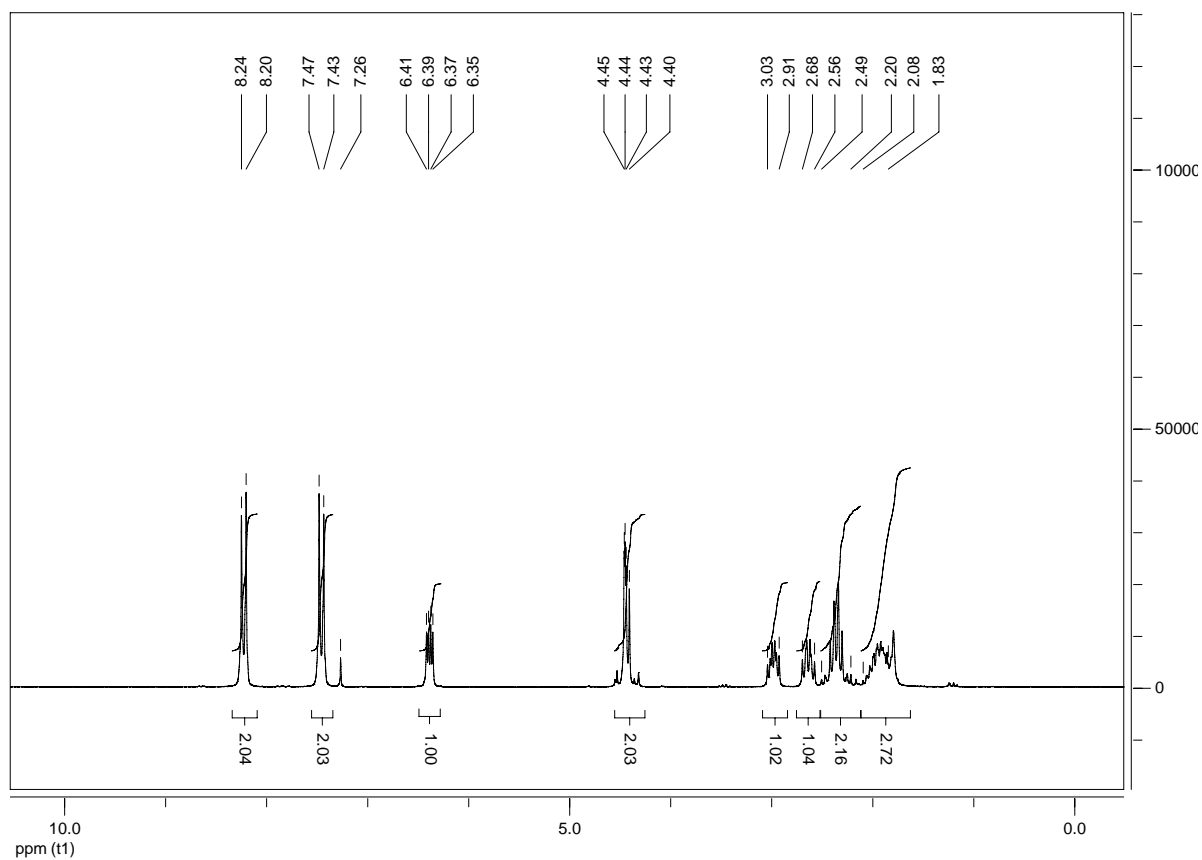
$^{13}\text{C}$  NMR (50 MHz,  $(\text{CD}_3)_2\text{SO}$ ):



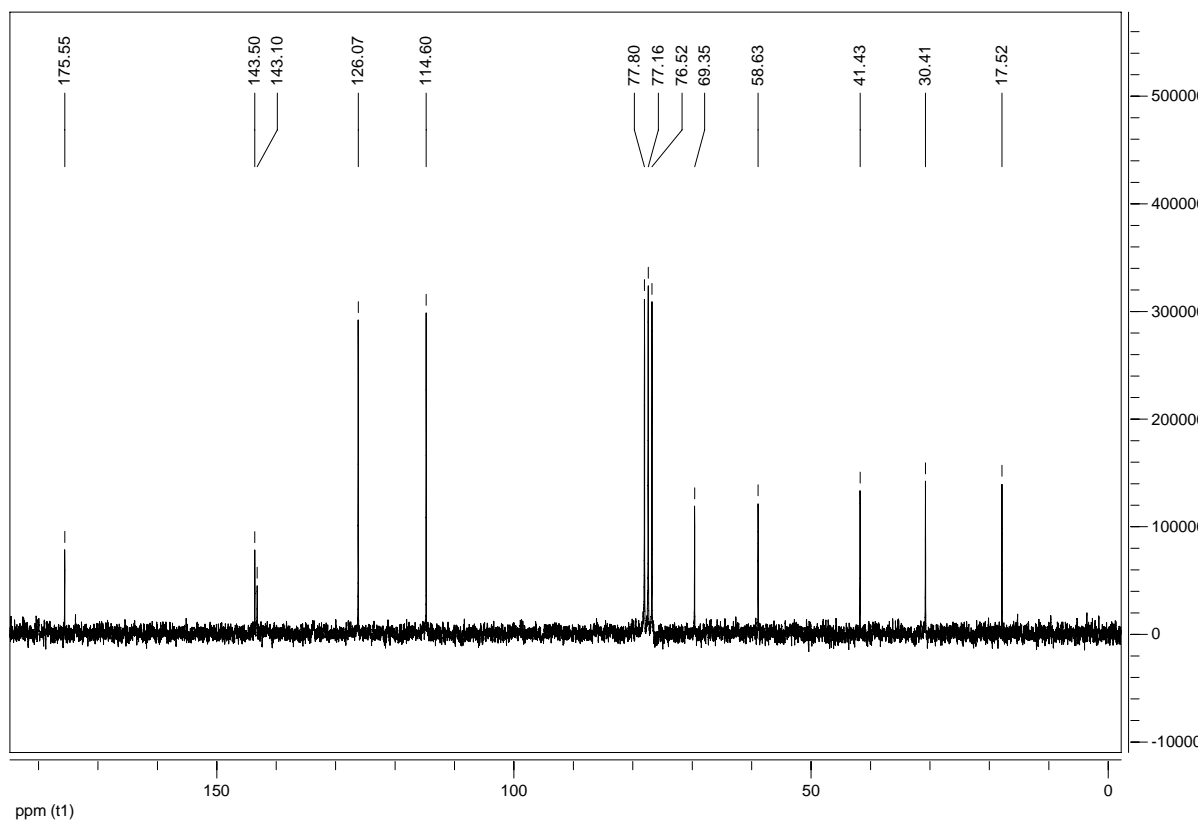


### Compound 10

$^1\text{H}$  NMR (200 MHz,  $\text{CDCl}_3$ ):



$^{13}\text{C}$  NMR (50 MHz,  $\text{CDCl}_3$ ):



## X-Ray diagrams

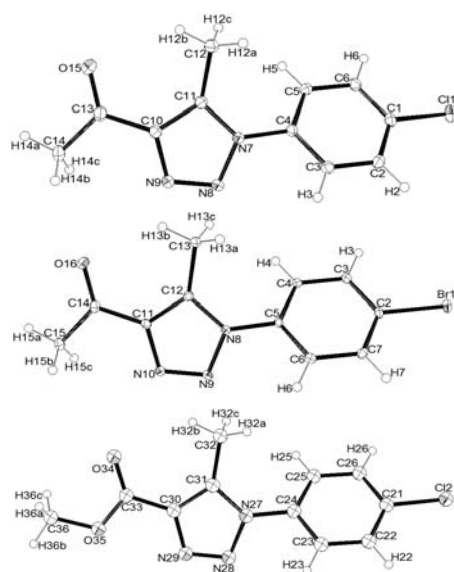


**Fig. 1** ORTEP diagrams (30% probability) of cycloadducts **3b,c**, and **3f**.

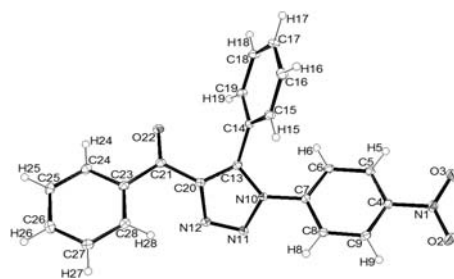


**Fig. 2** ORTEP diagram (30% probability) of cycloadduct **5a**.